Protein Expression and Function of Organic Anion Transporters in Short-Term and Long-Term Cultures of Huh7 Human Hepatoma Cells

Melina M. Malinen[a,b], **Katsuaki Ito**[a,c], **Hee Eun Kang**[a,d], **Paavo Honkakoski**[b], and **Kim L. R. Brouwer**[a,*]

[a]Division of Pharmacotherapy and Experimental Therapeutics, UNC Eshelman School of Pharmacy, University of North Carolina at Chapel Hill, Chapel Hill, North Carolina, USA [b]School of Pharmacy, Faculty of Health Sciences, University of Eastern Finland, Kuopio, Finland [c]DMPK Research Department, Teijin Pharma Limited, Hino, Tokyo, Japan [d]College of Pharmacy and Integrated Research Institute of Pharmaceutical Sciences, The Catholic University of Korea, Bucheon, South Korea

Abstract

Human-derived hepatic cell lines are a valuable alternative to primary hepatocytes for drug metabolism, transport and toxicity studies. However, their relevance for investigations of drug-drug and drug-organic anion (e.g., bile acid, steroid hormone) interactions at the transporter level remains to be established. The aim of the present study was to determine the suitability of the Huh7 cell line for transporter-dependent experiments. Huh7 cells were cultured for 1 to 4 weeks and subsequently were analyzed for protein expression, localization and activity of solute carrier (SLC) and ATP-binding cassette (ABC) transporters involved in organic anion transport using liquid chromatography-tandem mass spectroscopy, immunocytochemistry, and model substrates [^{3}H]taurocholate (TCA), [^{3}H]dehydroepiandrosterone sulfate (DHEAS) and 5 (and 6)-carboxy-2', 7'-dichlorofluorescein (CDF) diacetate. The extended 4-week culture resulted in a phenotype resembling primary hepatocytes and differentiated HepaRG cells: cuboidal hepatocyte-like cells with elongated bile canaliculi-like structures were surrounded by epithelium-like cells. Protein

[*]**Corresponding author** Kim L. R. Brouwer, Pharm.D., Ph.D., UNC Eshelman School of Pharmacy, University of North Carolina at Chapel Hill, CB# 7569, Chapel Hill, NC 27599-7569, Phone: (919) 962-7030, Fax: (919) 962-0644, kbrouwer@unc.edu.

expression of OSTα, OSTβ and OATP1B3 increased over time. Moreover, the uptake of the SLC probe substrate DHEAS was higher in 4-week than in 1-week Huh7 cultures. NTCP, OATP1B1, BSEP and MRP3 were barely or not detectable in Huh7 cells. OATP2B1, MRP2 and MRP4 protein expression remained at similar levels over the four weeks of culture. The activity of MRP2 and the formation of bile canaliculi-like structures were confirmed by accumulation of CDF in the intercellular compartments. Results indicate that along with morphological maturation, transporters responsible for alternative bile acid-secretion pathways are expressed and active in long-term cultures of Huh7 cells, suggesting that differentiated Huh7 cells may be suitable for studying the function and regulation of these organic anion transporters.

Keywords

ATP-binding cassette proteins; Huh7 cell line; Hepatocytes; Mass spectrometry; Membrane transport proteins; Phenotype; Solute carrier proteins

1. INTRODUCTION

Human-derived hepatic cell lines such as HepG2, Huh7 and HepaRG are widely used tools to study metabolism and toxicity of substances because they are an economical and reproducible model as compared to human primary hepatocytes. However, the protein expression of drug-metabolizing enzymes and drug transporters in these hepatic cell lines is sometimes aberrant. For example, protein expression of the major drug-metabolizing enzyme, cytochrome P450 (CYP) 3A4, is ~90% lower in HepG2 and Huh7 cells than in primary human hepatocytes (Shi et al., 2018; Sison-Young et al., 2015), whereas CYP3A4 protein expression is significantly higher in HepaRG cells than in primary hepatocytes (Sison-Young et al., 2015). One of the most abundant hepatic uptake transporters, organic anion transporting polypeptide (OATP)1B1, is at least 2-fold lower in Huh7, HepaRG and HepG2 cells than in hepatocytes (Shi et al., 2018; Sison-Young et al., 2015; Wisniewski et al., 2016). Neither OATP1B3 nor sodium taurocholate cotransporting polypeptide (NTCP) are present in HepG2 cells (Wisniewski et al., 2016). The most abundant hepatic efflux transporter, bile salt export pump (BSEP), is 10-100-fold lower in HepG2 and HepaRG cells than in primary hepatocytes (Sison-Young et al., 2015; Wisniewski et al., 2016). In contrast, multidrug resistance-associated protein (MRP)2 is expressed in HepG2, Huh7 and HepaRG cells at levels close to primary hepatocytes (Shi et al., 2018; Sison-Young et al., 2015). Also, MRP3 is present in HepG2 and HepaRG cells (Sison-Young et al., 2015). These alterations in the expression of enzymes and transporters often limit the utility of the cell lines in accurately predicting drug-drug interactions, routes of drug metabolism, and transporter-dependent disposition of endogenous and drug metabolites (Bachour-El Azzi et al., 2015; Godoy et al., 2013; Le Vee et al., 2006).

Modifications to culture conditions have resulted in significant improvements in the gene expression profiles, and the metabolic and transporter function of the hepatic cell lines. As described above, HepG2 cells cultured in a standard 2D format express low levels of CYP enzymes (Shi et al., 2018; Sison-Young et al., 2015; Wilkening et al., 2003) and poor efflux transport activity (Cooper et al., 1994; Kubitz et al., 2004). However, the enzyme content

and the transport activity of HepG2 cells have been induced by culturing the cells in a 3D format with different extracellular matrices such as peptide or Matrigel hydrogels (Malinen et al., 2012; Ramaiahgari et al., 2014). Recent analyses of HepG2 cells suggest that these changes are more likely due to the extended culture period, allowed and supported by the 3D culture matrix, rather than the effect of the 3D format alone (Luckert et al., 2017).

Addition of 2% dimethyl sulfoxide (DMSO) during the differentiation of HepaRG cells is required to increase some CYP enzymes and maintain transporter levels (Antherieu et al., 2010). A high DMSO concentration also has enhanced the hepatic phenotype of Huh7 cells (Choi et al., 2009). However, DMSO does not seem necessary for the maturation of Huh7 cells, because the long-term cultures with and without DMSO showed comparable gene expression profiles for drug-metabolizing enzymes (Sivertsson et al., 2010). The same group also reported significant expression of various transporter mRNAs in confluent Huh7 cells cultured for four weeks (Sivertsson et al., 2013). For instance, the expression of BSEP (ABCB11), P-glycoprotein (ABCB1) and OATP1B1 (SLCO1B1) mRNAs was elevated, whereas transcripts of MDR3 (ABCB4), MRP2 (ABCC2), NTCP (SLC10A1), OATP1A2 (SLCO1A2) and OCT1 (SLC22A1) were unchanged.

These findings suggest that it might be possible to restore and/or maintain transporter expression and function by extending the culture time of Huh7 cells. However, to the best of our knowledge, there are no reports on functional drug or bile acid transport studies using differentiated Huh7 cells. Therefore, the aim of this study was to characterize protein expression and localization of organic anion transporters in short-term and long-term cultures of Huh7 cells. Investigations included immunocytochemical staining and proteomic analyses of the uptake (NTCP, OATP1B1 and OATP2B1), efflux (MRP2, BSEP, MRP3 and MRP4), and the bidirectional OSTα/β transporters. In addition, transport studies were performed with [^{3}H]taurocholate (TCA) (a substrate of NTCP, OATP1B1, OATP1B3, OATP2B1, OSTα/β, MRP3, and BSEP), [^{3}H]dehydroepiandrosterone sulfate (DHEAS) (a substrate of OATP1B1, OSTα/β, MRP2, MRP3, and MRP4) and 5(6)-carboxy-2',7'-dichlorofluorescein (CDF; a substrate of MRP2 and MRP3) diacetate.

2. MATERIALS AND METHODS

2.1. Compounds

[^{3}H]DHEAS (60 Ci/mmol, radiochemical purity > 97%), and [^{3}H]TCA; 9.7-15.4 Ci/mmol, radiochemical purity > 97%) were purchased from PerkinElmer Life Sciences (Boston, MA). DHEAS and TCA were obtained from Sigma-Aldrich (St. Louis, MO), and were dissolved in DMSO (Fisher Scientific, Fair Lawn, NJ). The stable isotope labeled peptides were generated by a peptide synthesis platform (PEPscreen®, Custom Peptide Libraries, Sigma-Genosys). All the other compounds were purchased from Fisher Scientific and Sigma-Aldrich and were the highest grade available.

2.2. Huh7 cell cultures

The human hepatoma Huh7 cell line (JCRB0403) was obtained from Sekisui Xenotech (Kansas City, KS) and cultured in maintenance medium [Dulbecco's modified Eagle's

medium (11995-092, Thermo Fisher Scientific, Waltham, MA)]. The medium was supplemented with 10% fetal bovine serum, 2 mM L-glutamine, 100 U/ml penicillin and 100 μg/mL streptomycin (all from Thermo Fisher Scientific)] at 37°C in a 5% CO_2 atmosphere. The Huh7 cells were seeded in microplates or flasks, as detailed below, at a density of 40,000 cells/cm^2 and were maintained from 7 to 28 days; the maintenance medium was renewed every 2 to 3 days. Confluency was reached at culture day 3, and cultures remained confluent at the time of analysis (day 7, 14, 21 or 28). The identity of the Huh7 cell line was verified by amplification of 17 short tandem repeats by the Cell Line Authentication Service of the American Type Culture Collection (ATCC, Manassas, VA).

2.3. Immunocytochemistry of transport proteins in Huh7 cells and human hepatocytes

Immunocytochemical staining was performed as described previously (Malinen et al., 2018) with minor modifications. Cryopreserved human hepatocytes (Lot HU8239, Thermo Fisher Scientific; Lot HUM4082B and Lot HUM4040 Lonza BioResearch, Durham, NC) were plated in glass bottom culture petri dishes (P35G-0-14-C, MatTek Corporation, Ashland, MA) previously coated with type I collagen (1.5 mg/ml in Hanks' balanced salt solution (HBSS), Corning Inc., Corning, NY) at a density of 0.45×10^6/cm^2. Twenty hours after the plating, hepatocytes were overlaid with 0.25 mg/ml Matrigel matrix (Corning Inc.) and cultured for 4 days as reported (Malinen et al., 2018). Huh7 cells were cultured in glass bottom 24-well plates (P24G-1.0-10-F, MatTek Corporation) from 7 to 28 days as described above. After fixation, permeabilization and blocking, the cells were incubated overnight with a primary antibody against human transporters, anti-BSEP (Abcam, Cambridge, UK; ab140616, diluted 1:50), anti-NTCP (Abcam, ab131084, diluted 1:50), anti-MRP2 (Kamiya Biomedical Co., Seattle, WA; MC-206, diluted 1:20), anti-MRP3 (Santa Cruz Biotechnology, Dallas, TX; sc-5774, diluted 1:50), anti-MRP4 (Sigma-Aldrich HPA002476, diluted 1:50), anti-OATP1B (Everest Biotech Ltd, Bicester, UK; EB10666, diluted 1:50), anti-OATP2B1 (Santa Cruz Biotechnology; sc-135099, diluted 1:50), anti-OSTα (Abcam; ab103442, diluted 1:50), or anti-OSTβ (Sigma-Aldrich HPA008533, diluted 1:50) in phosphate buffered saline (PBS) containing 5% fetal bovine serum and 0.2% bovine serum albumin. Alexa Fluor® 488-labeled secondary antibody was diluted 1:200 and incubated overnight with the cells. After washing, filamentous actin and nuclei were stained with Alexa Fluor® 594-labeled phalloidin (Thermo Fisher Scientific) and DAPI (4',6-diamidino-2-phenylindole dihydrochloride; Thermo Fisher Scientific), respectively. Stained cultures were mounted in ProLong Gold antifade reagent (Thermo Fisher Scientific) and analyzed using a LSM 710 confocal laser scanning microscope (Carl Zeiss Microscopy, LLC, Thornwood, NY). Image files were processed with ImageJ (Schneider et al., 2012). No deconvolution was applied.

2.4. Membrane protein extraction from Huh7 cells and human hepatocytes

Huh7 cells cultured in T75 flasks with tissue culture-treated surface (83.3911.002, Sarstedt, Newton, NC) for 1, 2, 3, and 4 weeks (n = 3-4 each) were rinsed twice with ice-cold Tris-buffered saline and the membrane proteins were isolated using ProteoExtract™ Native Membrane Protein Extraction Kit (Calbiochem®, EMD Biosciences, Inc. Darmstadt, Germany) according to the manufacturer's protocol for adherent cells. The pellets of cryopreserved human hepatocytes (8.4×10^6 cells, Lot HUP1001; 10-donor pool, Lonza

BioResearch) were processed with the Membrane Protein Extraction kit by following the manufacturer's protocol for suspension cells. Total proteins were measured with Pierce™ BCA Protein assay kit (Thermo Fisher Scientific) and the samples were stored at −80°C until further use.

2.5. Preparation of samples for LC-MS/MS-based proteomic analysis

Prior to the liquid chromatography-tandem mass spectrometry (LC-MS/MS)-based proteomic analysis, the membrane protein samples were processed by protease digestion. Briefly, 100 μg of each membrane protein sample was mixed in ammonium bicarbonate buffer (25 mM) containing 5% deoxycholate and 10 mM dithiothreitol, followed by incubation at 56°C for 40 min. Then, iodoacetamide was added to achieve a final concentration of 15 mM, and the sample was incubated at room temperature for 30 min. The sample was diluted 5-fold with ammonium bicarbonate buffer and processed by protease digestion using Lys-C protease followed by trypsin. First, Lys-C protease (Thermo Fisher Scientific) was added to the sample to achieve a protein:protease ratio of 20:1. After incubation at 37°C for 4 hr, trypsin was added to a protein:trypsin ratio of 20:1 followed by incubation at 37°C overnight. The protease reaction was stopped by adding formic acid to a final concentration of 2% (v/v). The mixture of stable isotope-labeled peptides (Supplementary Table 1) was added as internal standards. The sample was processed with solid phase extraction using Oasis HLB (Waters Co., Milford, MA). Briefly, the cartridge was rinsed with methanol and equilibrated with 0.1% formic acid in water (v/v), and the sample was passed through the cartridge. After rinsing the cartridge with 0.1% formic acid in water (v/v), the peptides were eluted by 0.1% formic acid in acetonitrile (v/v). The eluate was evaporated using a centrifugal evaporator and reconstituted in 0.1% formic acid and 2% acetonitrile in water (v/v/v). After centrifugation (21,000 g, 1 min), the supernatant was analyzed by LC-MS/MS.

2.6. LC-MS/MS-based proteomic analysis for transport proteins

Unique signature peptides were selected for quantification of each transporter (Supplementary Table 1) based on literature reports (Li et al., 2008; Prasad et al., 2014; Uchida et al., 2011; Wang et al., 2015) and previously reported criteria (Prasad and Unadkat, 2014). The peptides were analyzed by LC-MS/MS [Thermo Scientific™ TSQ Quantum Ultra Triple Quadrupole mass spectrometer (Thermo Fisher Scientific) with nanoAcquity UPLC (Waters Co., Milford, MA)] in the selected reaction monitoring (SRM) mode with four sets of transitions. Membrane protein samples were injected onto the Waters® ACQUITY UPLC M-Class Symmetry C18 Trap Column (5 μm, 180 μm × 20 mm, Waters Co.) at a flow rate of 5 μL/min in 98% mobile phase A (0.1% formic acid in water) and 2% B (0.1% formic acid in acetonitrile) for 3 min. After trapping, the peptides were separated on an analytical column (Waters® ACQUITY UPLC HSS T3 nanoACQUITY Column, 1.8 μm, 100 μm × 100 mm, Waters Co.) at a flow rate of 0.6 μL/min, and a linear gradient of mobile phase B at a concentration of 5% for 0-1 min, 5-35% for 1-25 min, 35-90% for 25-25.5min, followed by the washing step using 90% mobile phase B for 4.5 min, and re-equilibrium for 10 min. Before the measurements, the multiple reaction monitoring transitions for each peptide were determined from MS/MS spectra. The collision energies were optimized to maximize signal strength. The data were processed by integrating the

peak areas generated from the reconstructed ion chromatograms for the analyte peptides and their respective internal standards using Xcalibur software (Thermo Fisher Scientific). When analyte peaks were detected in three or four sets of transitions, the transporters were considered to be expressed, and then the peak area ratios of the analyte peptide to its internal standard were calculated for three or four sets of transitions. To compare the expression levels of transporters among samples, the peak area ratio from the transitions for each peptide was averaged and compared to those in the reference sample (depending on transporter expression, either 10-donor pool of human hepatocytes or 1-week cultures of Huh7 cells). Due to the relative LC-MS/MS quantitation, the accuracy of the method was not calculated. The repeatability was evaluated by multiple measurements of the reference sample (hepatocytes), indicated as standard deviation (SD) and coefficient of variation (CV %) in Figure 2 and Supplementary Table 2.

2.7.   Uptake in Huh7 cells

Huh7 cells cultured in 24-well plates with tissue culture-treated surface (353226, Thermo Fisher Scientific) for 7 or 28 days were washed twice and pre-incubated for 10 min at 37°C with extracellular fluid (ECF Na$^+$) [122 mM sodium chloride (NaCl), 25 mM KHCO$_3$, 3 mM KCl, 0.4 mM KH$_2$PO$_4$, 10 mM D-glucose, 1.4 mM CaCl$_2$, 1.2 mM MgSO$_4$, and 10 mM HEPES (pH 7.4)] or ECF where 122 mM NaCl was replaced by 122 mM choline chloride (C$_5$H$_{14}$ClNO, CholCl) (ECF Chol$^+$) (Uchida et al., 2011). Transport was initiated by addition of uptake buffer containing a test substrate (10 μM of unlabeled TCA or 2.5 μM of unlabeled DHEAS, and 200-300 nCi/mL of [^{3}H]-labeled substrate). TCA was used to measure the activity of NTCP, OATP1B1, OATP1B3, OATP2B1, OSTα/β, MRP3, and BSEP, whereas DHEAS was used to evaluate the function of OATP1B1, OSTα/β, MRP2, MRP3, and MRP4 (Abe et al., 2001; Artursson et al., 2013; Hsiang et al., 1999). To detect uptake, the transport was stopped after 2 min by washing with ice-cold buffer. The cells were solubilized in lysis buffer (0.5% Triton X-100, 0.005% Antifoam-A in PBS, pH 7.4).

Lysates were analyzed in scintillation vials (Research Products International Corp., Mt Prospect, Il) using Bio-Safe II counting fluid (Research Products International Corp., Mt Prospect, IL) in a Tri-Carb 3100TR liquid scintillation counter (PerkinElmer Inc.). The amount of substrate transported into the cells or buffer was normalized to the total protein of the corresponding cell cultures (Pierce BCA™ protein assay kit, Thermo Fisher Scientific).

2.8.   Canalicular efflux in Huh7 cells

Formation of bile canaliculi-like structures and canalicular efflux activity was measured with CDF diacetate, a marker of efflux transport in hepatocytes (Zamek-Gliszczynski et al., 2003), as described previously (Tian et al., 2004). Huh7 cells cultured in a glass bottom 24-well plate (MatTek Corporation) were exposed to CDF diacetate at a final concentration of 2 μM for 10 min at 37 °C. The nuclei were visualized by addition of DAPI at a final concentration of 5 μM in the incubation buffer with CDF. After washing with standard HBSS, the disposition of fluorescent CDF and DAPI was observed with a LSM 710 confocal laser-scanning microscope (Carl Zeiss Microscopy), and the images were processed with ImageJ.

2.9. Data analysis

Data are presented as mean and standard deviation (SD). All data were analyzed by a 1-way or 2-way ANOVA, either with Dunnett's or Sidak's multiple comparisons test, respectively, using Prism 7 (GraphPad Software Inc., La Jolla, CA).

3. RESULTS

3.1. Hepatocyte-like morphology is established in Huh7 cells over time in culture

During the proliferation phase, Huh7 cells appeared as a homogeneous cell population with an epithelial phenotype showing no regular structural organization. Once the cells reached confluency, they underwent morphological changes and took on the appearance of cuboidal, hepatocyte-like cells and spherical actin filament bundles (*i.e.*, bile canaliculi-like structures) (Fig. 1A). After 4 weeks of culture, the cells had organized into two different clusters (Fig 1B). The high, multilayered clusters displayed a typical hepatocyte-like morphology with many elongated bile canaliculi-like structures (hepatic trabeculae) (Fig 1B and 1C), whereas the flat areas around the cuboidal cell clusters resembled epithelium-like cells (Fig. 1D).

3.2. Expression of transport proteins in Huh7 cells

The impact of extended culture time on the expression of organic anion transporters in Huh7 cells was monitored using mass spectrometer-based proteomic analysis and was compared to human hepatocytes. Overall, the protein expression of transporters was lower in Huh7 cell cultures than in human hepatocytes (Fig. 2). The main hepatic bile acid uptake transporter, NTCP, was not detected in Huh7 cells, whereas it was detected in human hepatocytes. However, the organic anion uptake transporters, OATP1B3 and OATP2B1, were detected in Huh7 cells although the expression level was lower than human hepatocytes. OATP2B1 was detected in Huh7 cells after 1 week of culture, while OATP1B3 was detected after 3 weeks of culture. Interestingly, OATP1B1, which was detected in human hepatocytes was not detected in Huh7 cells even after 4 weeks of culture. BSEP, the main hepatic bile acid efflux transporter, was not detected in Huh7 cell cultures, whereas MRP2 was detected in 1-week Huh7 cells and remained at approximately the same level over 4 weeks. As expected, MRP4 and OSTα were not detected in human hepatocytes, but they were detected in Huh7 cells. The expression of OSTα increased over the culture time and was at the highest level after 4 weeks of culture. MRP3 was not detected in either Huh7 cell cultures or human hepatocytes (data not shown). Na^+/K^+-ATPase increased over the culture time, along with the total protein content in Huh7 cell cultures (data not shown).

3.3. Localization of transport proteins in Huh7 cells

The expression and localization of organic anion transporters in Huh7 cells cultured for 1-week and 4-weeks were assessed by immunocytochemistry. The expression of OSTα/β subunits, OSTα and OSTβ, was markedly higher in 4-week than 1-week cultured Huh7 cells (Fig. 3). The majority of the cells expressed OSTα and OSTβ at the plasma membranes in 4-week cultures (Fig. 3 and Fig. 4). OSTα and OSTβ were present on the plasma membrane only in some Huh7 cells after 1 week, while OATP2B1 was detected already in 1-week cultures (Fig. 3). Expression of OATP1B (but not OATP2B1) seemed to increase over the

culture time (Fig. 3) and in 4-week cultures OSTα, OSTβ, OATP1B and OATP2B1 were abundant at the plasma membranes (Fig. 4). The expression of the main hepatic bile acid uptake transporter, NTCP, and the main hepatic bile acid efflux transporter, BSEP were low or missing in both 1- and 4-week cultured Huh7 cells (Fig. 3 and Fig. 5). In contrast, MRP2 and MRP4 expression was distinct already in 1-week cultures (Fig. 5). MRP2 was localized at the F-actin bundles of hepatocyte-like cell clusters, whereas MRP4 was abundant in the flattened epithelium-like cells (Fig. 4). MRP3 appeared to be localized in intracellular domains (Fig. 5).

3.4. TCA and DHEAS uptake in Huh7 cells

Uptake of the model substrates, TCA and DHEAS, was measured in Huh7 cells cultured for 1 week and 4 weeks. The assay was performed both in standard sodium buffer (ECF Na$^+$) and in low sodium buffer (ECF Chol$^+$) to distinguish the function of the Na$^+$-dependent organic anion uptake transporter, NTCP, from the Na$^+$-independent organic anion transporters (OATPs and OSTα/β) (Fig. 6). Notably, uptake of TCA and DHEAS was higher in low sodium buffer as compared to standard buffer in 1-week cultures of Huh7 cells. When the assay was performed in the standard buffer, TCA transport was similar in Huh7 cells cultured for 1 week and 4 weeks (Fig. 6A). However, in low sodium buffer, TCA uptake was higher in 1-week than 4-week cultures. In contrast, uptake of DHEAS, a substrate of OATPs and OSTα/β transporters, was significantly higher in 4-week than 1-week Huh7 cell cultures (Fig. 6B).

3.5. Functional polarity of Huh7 cells

Formation of functional bile canalicular structures was determined in 1-week and 4-weeks cultures of Huh7 cells using CDF as a model substrate (Fig. 7, Supplementary Fig. 1). CDF fluorescence accumulated into vesicle-like structures between adjacent cells reflecting the canalicular efflux of CDF and the presence of bile canaliculi-like structures with functional tight junctions in both 1-week and 4-week cultures. The canaliculi were spherical in 1-week cultures, whereas 4-week cultures contained CDF in both spherical and tubular structures. Since CDF is a substrate of MRP2, the accumulation confirms the canalicular localization and activity of MRP2. In fact, the CDF accumulation (Fig. 7, Supplementary Fig. 1) resembles the pattern observed in MRP2 immunocytochemistry (Fig. 5).

4. DISCUSSION

The common limitation of hepatoma cell lines for drug transport studies is their dedifferentiated phenotype and aberrant expression and function of transporters under standard culture conditions. The present study evaluated the effect of extended culture time on the protein expression, localization and function of organic anion transporters in the human Huh7 cell line. Maintaining confluent Huh7 cell cultures up to 4 weeks restored a hepatocyte-like morphology and induced the expression of some SLC family transport proteins. Moreover, the uptake of the SLC probe substrate DHEAS was higher in 4-week than in 1-week Huh7 cultures. These findings agree with the previous studies where extension of culture time induced the mRNA expression of multiple transcription factors, drug-metabolizing enzymes and some transporters in Huh7 cells (Sivertsson et al., 2013;

Sivertsson et al., 2010). However, the effect on the protein expression, localization or function of transporters was not investigated in these reports.

In the present study, confluent Huh7 cells cultured for several weeks formed cell clusters rich in bile canaliculi-like structures and cuboidal morphology. These cell clusters were reminiscent of primary hepatocyte cultures (Arterburn et al., 1995). The appearance of hepatocyte-like morphology indicates that it is possible to restore the original liver epithelial cell morphology of Huh7 cells (Nakabayashi et al., 1982) by modifying the culture conditions. However, the hepatocyte-like 4-week Huh7 cell clusters were surrounded by flattened cells, and this bimorphic phenotype highly resembled differentiated HepaRG cultures, where regions of flattened cells are also present amongst the hepatocyte-like cell clusters (Hoekstra et al., 2011; Jackson et al., 2016).

The protein expression of OATP1B3, OSTα and OSTβ was up-regulated (Fig. 2 and 3), whereas OATP2B1, MRP2 and MRP4 proteins remained at similar levels over the 4 weeks of culture. The constancy of MRP2 (ABCC2) mRNA in confluent Huh7 cell cultures has been reported previously (Sivertsson et al., 2010). The same study also showed that BSEP (ABCB11) and OATP1B1 (SLCO1B1) transporter mRNAs were increased over time. However, in the present study, BSEP and OATP1B1 proteins were not detected by proteomics; BSEP was expressed only in some cells, and overall at very low levels based on immunocytochemistry (Fig. 5). Similarly, the expression of BSEP protein was reported to be very low in HepG2 cells (Sison-Young et al., 2015; Wisniewski et al., 2016). To the best of our knowledge, the protein expression of BSEP has not been evaluated previously in Huh7 cells. The presence of OATP1B1 protein in Huh7 cells has been reported (Shi et al., 2018). However, Shi and colleagues used Huh7 microsomes in their analyses, whereas we analyzed Huh7 membrane protein fractions. The inducibility of OSTα (SLC51A) and OSTβ (SLC51B) gene expression in Huh7 cells has been reported previously (Landrier et al., 2006; Schaffner et al., 2015; Xu et al., 2014). The finding that OSTα and MRP4 proteins were not detected in the human hepatocytes was expected and in agreement with the previous proteomics analysis of human liver (Uhlen et al., 2015). Both OSTα and MRP4 proteins are expressed at low or undetectable levels in human liver (Uhlen et al., 2015), but are induced in cholestatic liver diseases (Boyer et al., 2006; Malinen et al., 2018; Thakkar et al., 2017).

Immunofluorescence was used to evaluate the localization of the transporters and to detect OSTβ, which was not analyzed by LC-MS/MS. OSTα, OSTβ, and OATP1B were at the plasma membranes after 4 weeks of culture, whereas OATP2B1, MRP2 and MRP4 were correctly localized at the plasma membranes already in 1-week cultures. MRP2 localized within the F-actin-rich canaliculi-like structures, whereas OSTα, OSTβ, OATP1B, OATP2B1, and MRP4 were detected on the basolateral membranes. The accumulation of CDF in the intercellular structures confirmed the correct localization of MRP2 at the canalicular membranes and also demonstrated the functionality of MRP2 in Huh7 cell cultures. MRP3 was detected only in intracellular compartments, in agreement with a previous report (Carrasco-Torres et al., 2016). This mislocalization of MRP3 may explain why it was not detected by LC-MS/MS where membrane protein fractions of Huh7 cells were analyzed. NTCP was not detected by LC-MS/MS or by immunofluorescence in Huh7 cells, in agreement with the finding in another hepatic cell line, HepG2 (Wisniewski et al.,

2016). Incidentally, NTCP was expressed in primary hepatocytes, but protein levels were the lowest among the uptake transporters (Wisniewski et al., 2016).

Despite up-regulation of OSTα/β and OATP1B transporters over time, the overall profile of organic anion transporters in Huh7 cells, even after 4 weeks in culture, was different from that in primary human hepatocytes. The absence of the main bile acid transporters NTCP and BSEP, combined with the strong expression of OSTα, OSTβ and MRP4, are distinct differences between Huh7 cells and primary human hepatocytes. This difference suggests that Huh7 cells could function as a cholestatic rather than a normal liver cell model (Chai et al., 2015; Thakkar et al., 2017). The lack of NTCP and BSEP, together with the downregulation of OATP1B1 and OATP1B3, probably decrease the transport of bile acids in Huh7 cells. The upregulation of OSTα/β and MRP4, which also occurs in patients with cholestasis, may lead to increased transport of steroid hormone and bile acid sulfates. The altered transporter expression in Huh7 cells may be due to the cancerous origin of the Huh7 hepatoma cells, as the MRP4 expression has been reported to be high in hepatocellular carcinoma (Borel et al., 2012). In addition, OATP1B1, OATP1B3, and OATP2B1 proteins were expressed at lower levels in all Huh7 cell cultures compared to primary human hepatocytes, also in agreement with previously published studies in hepatocellular carcinoma samples and HepG2 cells (Libra et al., 2006; Sison-Young et al., 2015; Vavricka et al., 2004).

The results of functional transport studies supported the notion that organic anion transporter expression is altered in long-term Huh7 cell cultures. The uptake of DHEAS, the model substrate of OATP1B1, OSTα/β, MRP2, MRP3 and MRP4 was higher in 4-week than 1-week cultures of Huh7 cells, and this seems to correlate with the increased expression of the OSTα/β transporter. The uptake of TCA in standard buffer, which reflects the combined net activity of NTCP, OATP1B1, OATP1B3, OATP2B1, OSTα/β, BSEP and MRP3, was at the same level in 1-week and 4-week cell cultures (Fig. 6A standard buffer). This finding was somewhat surprising, because NTCP and OATP1B1 proteins were not detected, OATP2B1 remained at a similar level, and the expression of OATP1B3 and OSTα/β was increased. A possible explanation for the invariable TCA uptake, despite increased transporter expression in 4-week Huh7 cell cultures, could be the bidirectional nature of OSTα/β and the low expression of TCA efflux transporters (BSEP and MRP3). Without efflux, TCA can only accumulate to a certain extent into Huh7 cells because further accumulation is prevented by the equilibrating nature of OSTα/β. In contrast, the constant expression of MRP2, the canalicular efflux transporter of DHEAS, allows transcellular movement of DHEAS from the extracellular compartment (buffer) into canalicular spaces. Therefore, the apparent uptake of DHEAS increases along with the increased expression of OSTα/β.

Increased cellular uptake of TCA and DHEAS in the low sodium (ECF Chol[+]) buffer suggests that removal of Na^+ ions could stimulate the uptake transporters. Decreased extracellular sodium may alter the intracellular proton (H^+) concentration by rendering the Na^+/H^+ exchanger inactive (Weintraub and Machen, 1989), which in turn can affect the activity of the OATP (Leuthold et al., 2009) as well as the OSTα/β transporters (Malinen et al., 2018). A similar phenomenon has been reported with HepG2 cells, where glycocholate uptake was higher in choline-containing than in sodium-containing buffer (Marin et al.,

2003). The authors explained their results in terms of intracellular acidification and a resulting change in the Na^+-independent uptake of glycocholate, most probably due to a change in OATP-mediated activity. However, our recent findings suggest that the elevated uptake in choline-containing buffer may be due to changes in intrinsic activity of OSTα/β (Malinen et al., 2018).

The mechanism of OATP1B3 and OSTα/β induction in long-term cultures of Huh7 cells may be due to the elevated expression of the nuclear receptors CAR, PXR, HNF4α and isoforms of RXR (Sivertsson et al., 2010). CAR has a binding site in the promoter of OSTβ (*SLC51B*) (Xu et al., 2014) and HNF4α is reported to upregulate OATP1B3 (*SLCO1B3*) and OSTα (*SLC51A*) genes (Knauer et al., 2013; Okuwaki et al., 2007). The induced transporters (OATP1B3 and OSTα/β) are also regulated by the bile acid receptor FXR. Although FXR mRNA was not elevated, its obligate partner RXR was induced in long-term cultures of Huh7 cells (Sivertsson et al., 2010). Overall, the expression of FXR has been reported to be higher in Huh7 cells than in human hepatocytes (Jouan et al., 2017). These findings indicate that the FXR pathway may be activated in confluent cultures of Huh7 cells. Also, other transcription factors such as Nrf2, aryl hydrocarbon receptor (AhR), liver X receptor alpha (LXRα) and the vitamin D receptor (VDR) may play a role in SLC transporter induction in Huh7 cells (Okuwaki et al., 2007; Shan et al., 2006). However, the expression of these transcription factors in the long-term confluent cultures of Huh7 cells has not been studied yet. Lack of OATP1B1, NTCP and BSEP proteins in the cultures of Huh7 cells may, most likely, relate to incomplete differentiation status of the cells. Alternatively, activation of the FXR and PXR pathways has been reported to down-regulate NTCP (Denson et al., 2001) and BSEP (Jigorel et al., 2006), respectively.

5. CONCLUSIONS

Long-term differentiated Huh7 cell cultures are a promising *in vitro* model to examine the hepatic disposition of drugs and endogenous compounds, particularly in cholestatic conditions when alternative bile acid transporters overtake the primary bile acid transporters. The appearance of a hepatic phenotype, resembling that of primary hepatocyte and HepaRG cell cultures, the presence of the ABCC family of transporters, and expression of several SLC transporters are advantageous, but the low levels of NTCP and BSEP expression are a major drawback. It should be noted that we did not test the effects of any medium supplements or extracellular matrix configurations in this study. Reports on the known inducers of differentiation and/or approaches to maintain a primary hepatocyte phenotype (Mork et al., 2012) suggest that treatments with insulin, glucocorticoids, or modifications in the extracellular matrices may provide cues to further develop a more human-like profile of transporter expression.

Supplementary Material

Refer to Web version on PubMed Central for supplementary material.

ACKNOWLEDGEMENTS

Abbreviations:

ABC	ATP-binding cassette
AhR	aryl hydrocarbon receptor
BSEP	bile salt export pump
ABCB	ATP-binding cassette subfamily B
ABCC	ATP-binding cassette subfamily C
ATPase	adenosine triphosphatase
CAR	constitutive androstane receptor
CDF	5 (6)-carboxy-2',7'-dichlorofluorescein
CholCl	choline chloride
CYP	cytochrome P450 enzyme
DAPI	4',6-diamidino-2-phenylindole
DHEAS	dehydroepiandrosterone sulfate
DMSO	dimethyl sulfoxide
ECF	extracellular fluid buffer
FXR	farnesoid X receptor
HBSS	Hanks' balanced salt solution
HNF4	hepatocyte nuclear factor-4
LC-MS/MS	liquid chromatography-tandem mass spectrometry
LXR	liver X receptor
MRP	multidrug resistance-associated protein
Nrf2	nuclear factor erythroid 2-related factor-2
OATP	organic anion transporting polypeptide
PBS	phosphate buffered saline
PXR	pregnane X receptor

RXR	retinoid X receptor
SLC	solute carrier transporter
NTCP	sodium taurocholate co-transporting polypeptide
OSTα/β	organic solute transporter alpha/beta
OATP	solute carrier organic anion transporter
SD	standard deviation
TCA	taurocholate
UGT	uridine 5'-diphospho-glucuronosyltransferase
VDR	vitamin D receptor

7. REFERENCES

Abe T, et al., 2001 Lst-2, a human liver-specific organic anion transporter, determines methotrexate sensitivity in gastrointestinal cancers. Gastroenterology 120, 1689–1699. [PubMed: 11375950]

Antherieu S, et al., 2010 Stable expression, activity, and inducibility of cytochromes p450 in differentiated heparg cells. Drug Metab. Dispos 38, 516–525. [PubMed: 20019244]

Arterburn LM, et al., 1995 A morphological study of differentiated hepatocytes in vitro. Hepatology 22, 175–187. [PubMed: 7601410]

Artursson P, et al., 2013 In vitro characterization of interactions with drug transporting proteins, in: Sugiyama Y, Steffansen B (Eds.), Transporters in drug development. Springer, New York, NY, AAPS Advances in the Pharmaceutical Sciences Series.

Bachour-El Azzi P, et al., 2015 Comparative localization and functional activity of the main hepatobiliary transporters in heparg cells and primary human hepatocytes. Toxicol. Sci. 145, 157–168. [PubMed: 25690737]

Borel F, et al., 2012 Adenosine triphosphate-binding cassette transporter genes up-regulation in untreated hepatocellular carcinoma is mediated by cellular micrornas. Hepatology 55, 821–832. [PubMed: 21932399]

Boyer JL, et al., 2006 Upregulation of a basolateral fxr-dependent bile acid efflux transporter ostalpha-ostbeta in cholestasis in humans and rodents. Am. J. Physiol. Gastrointest. Liver Physiol 290, G1124–1130. [PubMed: 16423920]

Carrasco-Torres G, et al., 2016 The transmembrane transporter abcc3 participates in liver cancer progression and is a potential biomarker. Tumour Biol 37, 2007–2014. [PubMed: 26337276]

Chai J, et al., 2015 Hepatic expression of detoxification enzymes is decreased in human obstructive cholestasis due to gallstone biliary obstruction. PLoS One 10, e0120055. [PubMed: 25798860]

Choi S, et al., 2009 Characterization of increased drug metabolism activity in dimethyl sulfoxide (dmso)-treated huh7 hepatoma cells. Xenobiotica 39, 205–217. [PubMed: 19280519]

Cooper AD, et al., 1994 Characteristics and regulation of bile salt synthesis and secretion by human hepatoma hepg2 cells. Hepatology 20, 1522–1531. [PubMed: 7982652]

Denson LA, et al., 2001 The orphan nuclear receptor, shp, mediates bile acid-induced inhibition of the rat bile acid transporter, ntcp. Gastroenterology 121, 140–147. [PubMed: 11438503]

Godoy P, et al., 2013 Recent advances in 2d and 3d in vitro systems using primary hepatocytes, alternative hepatocyte sources and non-parenchymal liver cells and their use in investigating mechanisms of hepatotoxicity, cell signaling and adme. Arch. Toxicol 87, 1315–1530. [PubMed: 23974980]

Hoekstra R, et al., 2011 The heparg cell line is suitable for bioartificial liver application. Int. J. Biochem. Cell Biol 43, 1483–1489. [PubMed: 21726661]

Hsiang B, et al., 1999 A novel human hepatic organic anion transporting polypeptide (oatp2). Identification of a liver-specific human organic anion transporting polypeptide and identification of rat and human hydroxymethylglutaryl-coa reductase inhibitor transporters. J. Biol. Chem. 274, 37161–37168. [PubMed: 10601278]

Jackson JP, et al., 2016 Contextualizing hepatocyte functionality of cryopreserved heparg cell cultures. Drug Metab. Dispos 44, 1463–1479. [PubMed: 27338863]

Jigorel E, et al., 2006 Differential regulation of sinusoidal and canalicular hepatic drug transporter expression by xenobiotics activating drug-sensing receptors in primary human hepatocytes. Drug Metab. Dispos 34, 1756–1763. [PubMed: 16837569]

Jouan E, et al., 2017 Drug transporter expression and activity in human hepatoma huh-7 cells. Pharmaceutics 9, 3.

Knauer MJ, et al., 2013 Transport function and transcriptional regulation of a liver-enriched human organic anion transporting polypeptide 2b1 transcriptional start site variant. Mol Pharmacol 83, 1218–1228. [PubMed: 23531488]

Kubitz R, et al., 2004 Trafficking of the bile salt export pump from the golgi to the canalicular membrane is regulated by the p38 map kinase. Gastroenterology 126, 541–553. [PubMed: 14762791]

Landrier JF, et al., 2006 The nuclear receptor for bile acids, fxr, transactivates human organic solute transporter-alpha and -beta genes. Am. J. Physiol. Gastrointest. Liver Physiol 290, G476–485. [PubMed: 16269519]

Le Vee M, et al., 2006 Functional expression of sinusoidal and canalicular hepatic drug transporters in the differentiated human hepatoma heparg cell line. Eur. J. Pharm. Sci 28, 109–117. [PubMed: 16488578]

Leuthold S, et al., 2009 Mechanisms of ph-gradient driven transport mediated by organic anion polypeptide transporters. Am J Physiol Cell Physiol 296, C570–582. [PubMed: 19129463]

Li N, et al., 2008 Absolute quantification of multidrug resistance-associated protein 2 (mrp2/abcc2) using liquid chromatography tandem mass spectrometry. Anal. Biochem 380, 211–222. [PubMed: 18558078]

Libra A, et al., 2006 Molecular determinants in the transport of a bile acid-derived diagnostic agent in tumoral and nontumoral cell lines of human liver. J. Pharmacol. Exp. Ther 319, 809–817. [PubMed: 16895978]

Luckert C, et al., 2017 Comparative analysis of 3d culture methods on human hepg2 cells. Arch. Toxicol 91, 393–406. [PubMed: 26872951]

Malinen MM, et al., 2018 Organic solute transporter ostalpha/beta is overexpressed in nonalcoholic steatohepatitis and modulated by drugs associated with liver injury. Am. J. Physiol. Gastrointest. Liver Physiol 314, G597–G609. [PubMed: 29420067]

Malinen MM, et al., 2012 Peptide nanofiber hydrogel induces formation of bile canaliculi structures in three-dimensional hepatic cell culture. Tissue Eng Part A 18, 2418–2425. [PubMed: 22712588]

Marin JJ, et al., 2003 Sensitivity of bile acid transport by organic anion-transporting polypeptides to intracellular ph. Biochim. Biophys. Acta 1611, 249–257. [PubMed: 12659967]

Mork LM, et al., 2012 Comparison of culture media for bile acid transport studies in primary human hepatocytes. J. Clin. Exp. Hepatol 2, 315–322. [PubMed: 25755453]

Nakabayashi H, et al., 1982 Growth of human hepatoma cells lines with differentiated functions in chemically defined medium. Cancer Res. 42, 3858–3863. [PubMed: 6286115]

Okuwaki M, et al., 2007 Lxr alpha transactivates mouse organic solute transporter alpha and beta via ir-1 elements shared with fxr. Pharm. Res 24, 390–398. [PubMed: 17177110]

Prasad B, et al., 2014 Interindividual variability in hepatic organic anion-transporting polypeptides and p-glycoprotein (abcb1) protein expression: Quantification by liquid chromatography tandem mass spectroscopy and influence of genotype, age, and sex. Drug Metab. Dispos 42, 78–88. [PubMed: 24122874]

Prasad B, Unadkat JD, 2014 Optimized approaches for quantification of drug transporters in tissues and cells by mrm proteomics. AAPS J 16, 634–648. [PubMed: 24752720]

Ramaiahgari SC, et al., 2014 A 3d in vitro model of differentiated hepg2 cell spheroids with improved liver-like properties for repeated dose high-throughput toxicity studies. Arch. Toxicol. 88, 1083–1095. [PubMed: 24599296]

Schaffner CA, et al., 2015 The organic solute transporters alpha and beta are induced by hypoxia in human hepatocytes. Liver Int 35, 1152–1161. [PubMed: 24703425]

Schneider CA, et al., 2012 Nih image to imagej: 25 years of image analysis. Nat Methods 9, 671–675. [PubMed: 22930834]

Shan Y, et al., 2006 Role of bach1 and nrf2 in up-regulation of the heme oxygenase-1 gene by cobalt protoporphyrin. FASEB J. 20, 2651–2653. [PubMed: 17065227]

Shi J, et al., 2018 Comparison of protein expression between human livers and the hepatic cell lines hepg2, hep3b, and huh7 using swath and mrm-hr proteomics: Focusing on drug-metabolizing enzymes. Drug Metab. Pharmacokinet 33, 133–140. [PubMed: 29610054]

Sison-Young RL, et al., 2015 Comparative proteomic characterization of 4 human liver-derived single cell culture models reveals significant variation in the capacity for drug disposition, bioactivation, and detoxication. Toxicol. Sci 147, 412–424. [PubMed: 26160117]

Sivertsson L, et al., 2013 Induced cyp3a4 expression in confluent huh7 hepatoma cells as a result of decreased cell proliferation and subsequent pregnane x receptor activation. Mol. Pharmacol. 83, 659–670. [PubMed: 23264496]

Sivertsson L, et al., 2010 Cyp3a4 catalytic activity is induced in confluent huh7 hepatoma cells. Drug Metab. Dispos 38, 995–1002. [PubMed: 20233841]

Thakkar N, et al., 2017 Effect of liver disease on hepatic transporter expression and function. J. Pharm. Sci 106, 2282–2294. [PubMed: 28465155]

Tian X, et al., 2004 Modulation of multidrug resistance-associated protein 2 (mrp2) and mrp3 expression and function with small interfering rna in sandwich-cultured rat hepatocytes. Mol. Pharmacol. 66, 1004–1010. [PubMed: 15385645]

Uchida Y, et al., 2011 Quantitative targeted absolute proteomics of human blood-brain barrier transporters and receptors. J. Neurochem. 117, 333–345. [PubMed: 21291474]

Uhlen M, et al., 2015 Proteomics. Tissue-based map of the human proteome. Science 347, 1260419. [PubMed: 25613900]

Vavricka SR, et al., 2004 The human organic anion transporting polypeptide 8 (slco1b3) gene is transcriptionally repressed by hepatocyte nuclear factor 3beta in hepatocellular carcinoma. J. Hepatol. 40, 212–218. [PubMed: 14739090]

Wang L, et al., 2015 Interspecies variability in expression of hepatobiliary transporters across human, dog, monkey, and rat as determined by quantitative proteomics. Drug Metab. Dispos 43, 367–374. [PubMed: 25534768]

Weintraub WH, Machen TE, 1989 Ph regulation in hepatoma cells: Roles for na-h exchange, cl-hco3 exchange, and na-hco3 cotransport. Am. J. Physiol 257, G317–327. [PubMed: 2551179]

Wilkening S, et al., 2003 Comparison of primary human hepatocytes and hepatoma cell line hepg2 with regard to their biotransformation properties. Drug Metab Dispos 31, 1035–1042. [PubMed: 12867492]

Wisniewski JR, et al., 2016 In-depth quantitative analysis and comparison of the human hepatocyte and hepatoma cell line hepg2 proteomes. J. Proteomics 136, 234–247. [PubMed: 26825538]

Xu S, et al., 2014 A novel raralpha/car-mediated mechanism for regulation of human organic solute transporter-beta gene expression. Am. J. Physiol. Gastrointest. Liver Physiol 306, G154–162. [PubMed: 24264050]

Zamek-Gliszczynski MJ, et al., 2003 Pharmacokinetics of 5 (and 6)-carboxy-2',7'-dichlorofluorescein and its diacetate promoiety in the liver. J. Pharmacol. Exp. Ther 304, 801–809. [PubMed: 12538836]
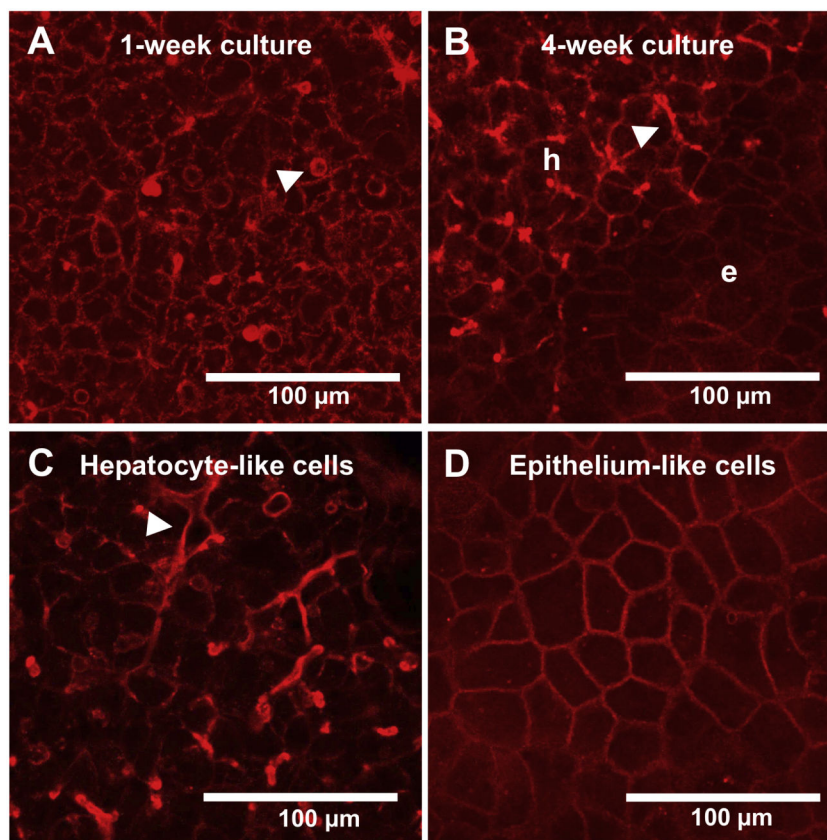
Figure 1.
Morphology of representative Huh7 cells maintained in culture for 7 days (A) or 28 days (B, C, D). Filamentous actin (F-actin) was stained with Alexa Fluor® 594-phalloidin (red). Hepatocyte-like cells and epithelium-like cells are indicated by "h" and "e", respectively. Accumulation of F-actin suggests the formation of bile canaliculi-like structures on the canalicular plasma membranes, indicated by a triangle.
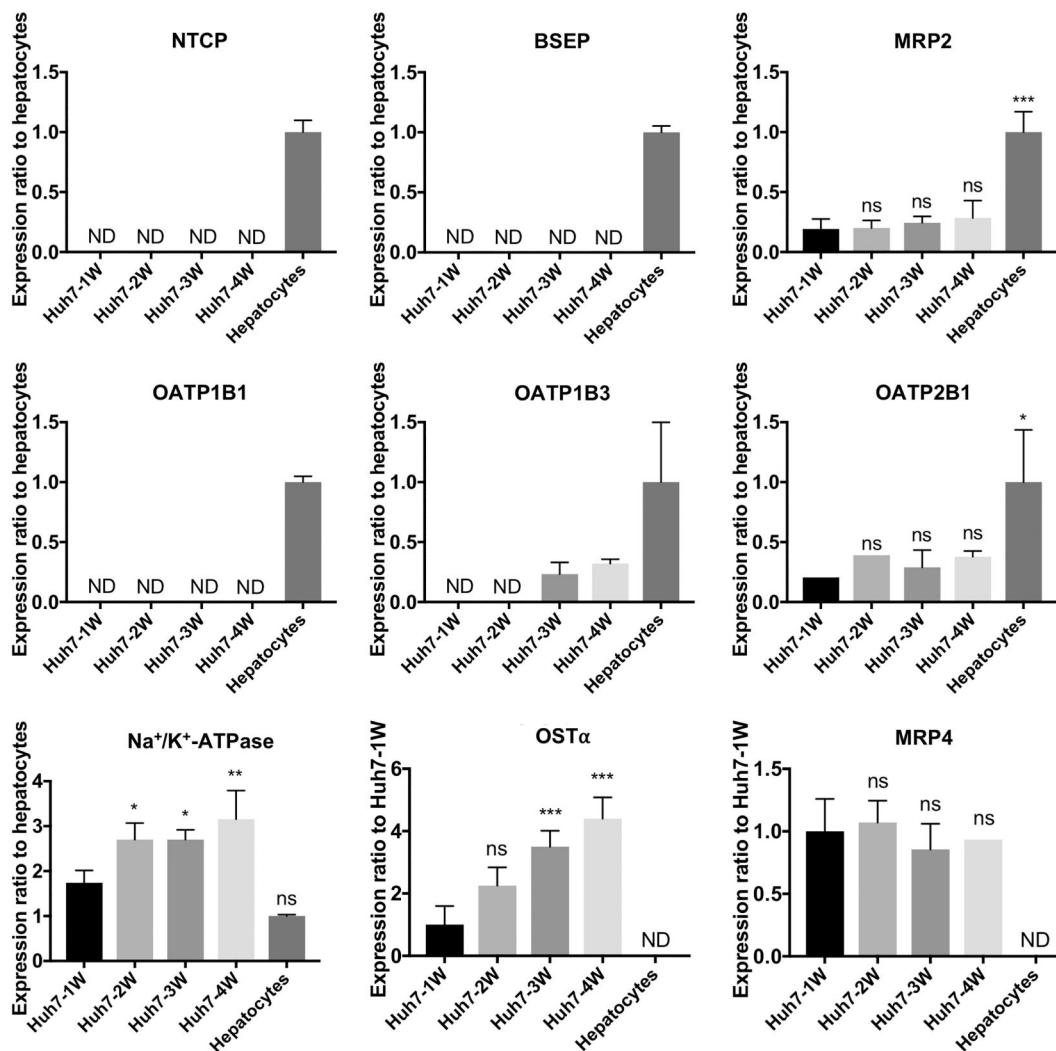
Figure 2.
Transporter protein expression in Huh7 cells and human hepatocytes measured by LC-MS/MS. Data represent mean ± SD (n=3-4 independent experiments, except n=2 for OATP2B1 Huh7-1W and Huh7-2W, and MRP4 Huh7-4W). When protein expression was detected in less than one-half of the samples in a group, the group is expressed as not detectable (ND). ns, not significant; *, $p<0.05$; **, $p<0.01$; ***, $p<0.001$, significantly different from Huh7 cells cultured for 1 week (Huh7-1W).
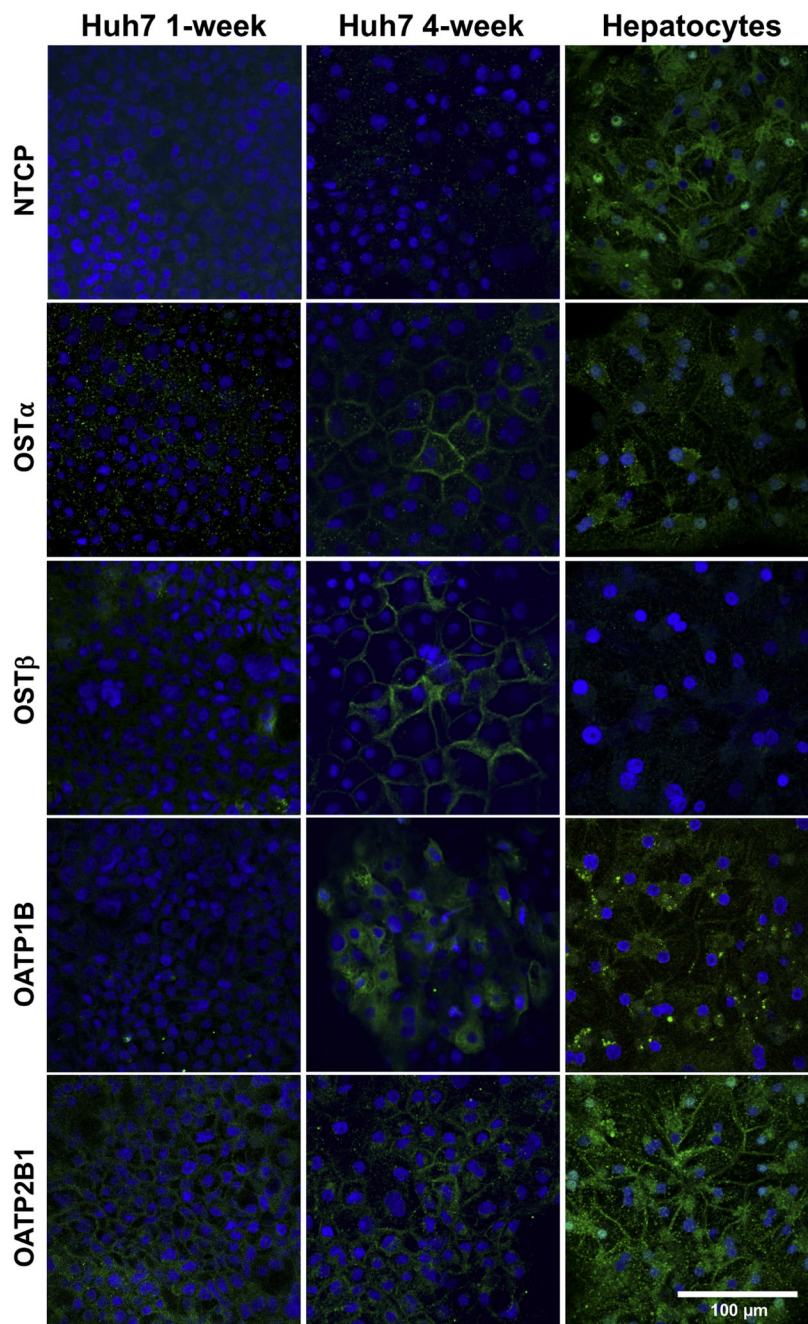
Figure 3.
Expression and localization of SLC transporters in representative Huh7 cells. Huh7 cells were cultured for 1 or 4 weeks, followed by immunostaining of transport proteins (green) with either anti-NTCP, anti-OSTα, anti-OSTβ, anti-OATP1B or anti-OATP2B1, and Alexa Fluor® 488-labeled secondary antibodies. Human hepatocytes were cultured in sandwich configuration for 5 days followed by immunostaining. Nuclei were visualized with DAPI (blue).
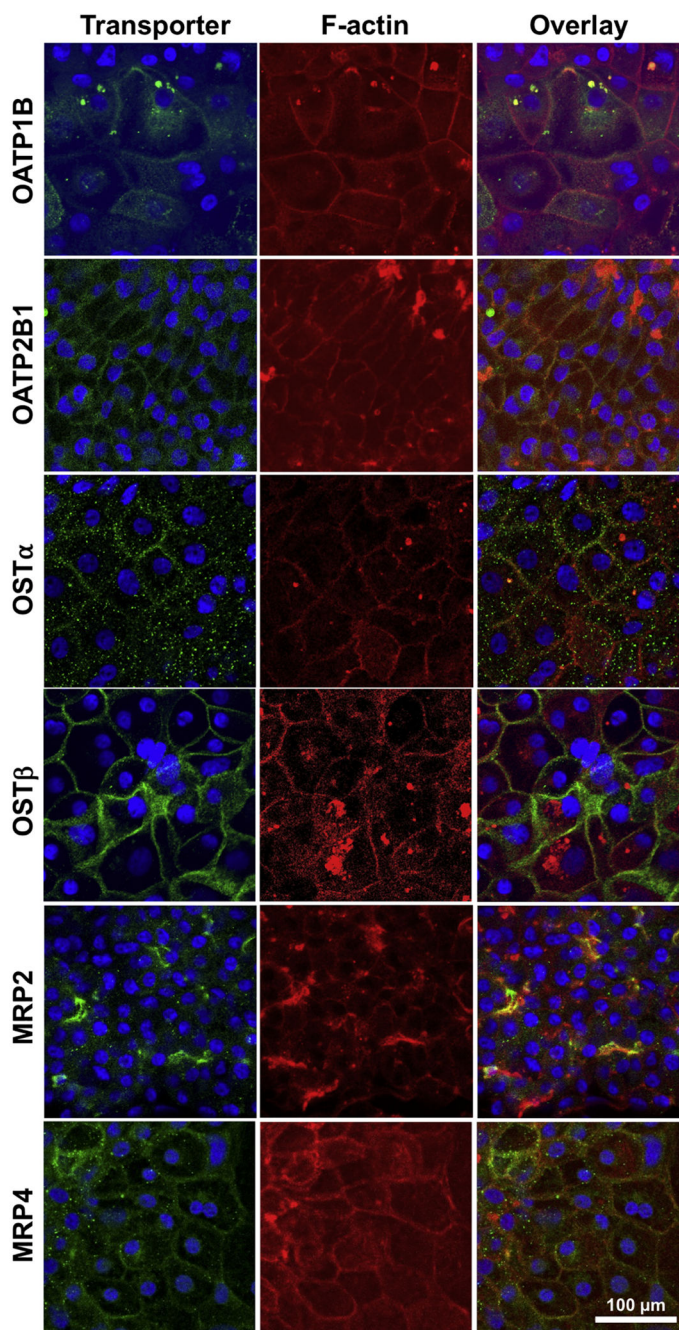
Figure 4.
Co-localization of transporters and filamentous actin (F-actin) in representative Huh7 cells cultured for 4 weeks. Transporters (green) were detected with anti-OATP1B, anti-OATP2B1, anti-OSTα, anti-OSTβ, anti-MRP2 and anti-MRP4 together with Alexa Fluor® 488-labeled secondary antibodies. Actin filaments and nuclei were visualized with Alexa Fluor® 594-labeled phalloidin (red) and DAPI (blue), respectively.
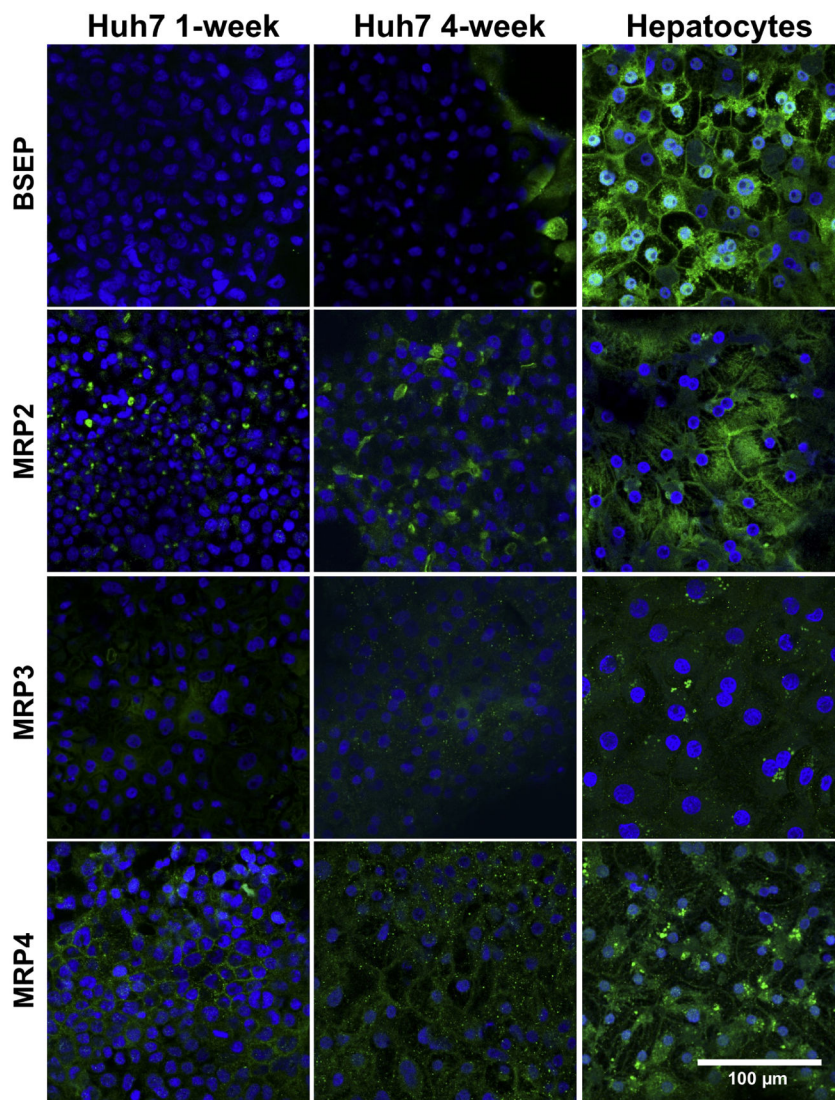
Figure 5.
Expression and localization of ABC transporters in representative Huh7 cells. Huh7 cells were cultured for 1 or 4 weeks, followed by immunostaining of transport proteins (green) with either anti-BSEP, anti-MRP2, anti-MRP3 or anti-MRP4, and Alexa Fluor® 488-labeled secondary antibodies. Human hepatocytes were cultured in sandwich configuration for 5 days followed by immunostaining. Nuclei were visualized with DAPI (blue).
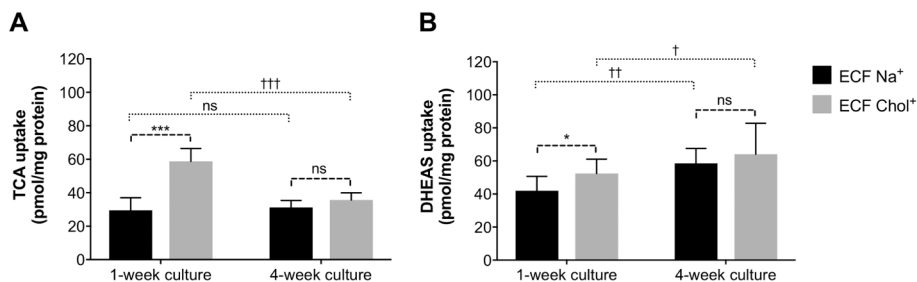
A

B

Figure 6.

Cellular uptake of TCA (A) and DHEAS **(B)** in 1-week and 4-week cultures of Huh7 cells. Cell cultures were treated with extracellular fluid (ECF-Na$^+$) or with extracellular fluid where sodium chloride was replaced with choline chloride (ECF-Chol$^+$) supplemented with TCA (10 μM and 300 nCi/mL) or DHEAS (2.5 μM and 300 nCi/mL) for 2 min, followed by washes, lysis and scintillation counting. Data represent mean ± SD (n=3 in triplicate). ns, not significantly different; *, p<0.05; ***, p<0.001 significantly different from ECF Na$^+$ buffer; †, p<0.05; ††, p<0.01; †††, p<0.001 significantly different from 1-week culture.
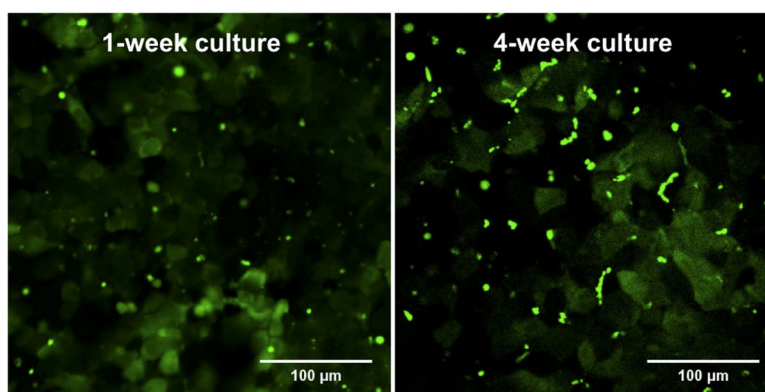
Figure 7.
Disposition of 5 (6)-carboxy-2',7'-dichlorofluorescein (CDF) (green) in 1-week and 4-week cultures of Huh7 cells. Huh7 cell cultures were treated for 10 min with 2 µM CDF diacetate, followed by washes with HBSS and confocal microscopy.